ACS APPLIED MATERIALS & INTERFACES

Research Article

www.acsami.org

Hair-Inspired Crystal Growth of HOA in Cavities of Cellulose Matrix via Hydrophobic–Hydrophilic Interface Interaction

Meng He,[†] Ryan T. K. Kwok,[‡] Zhenggang Wang,[†] Bo Duan,[†] Ben Zhong Tang,*[,‡] and Lina Zhang*[,†]

[†]Department of Chemistry, Wuhan University, Wuhan 430072, China

[‡]Department of Chemistry, Institute for Advanced Study, Division of Biomedical Engineering, Division of Life Science, State Key Laboratory of Molecular Neuroscience and Institute of Molecular Functional Materials, The Hong Kong University of Science and Technology, Clear Water Bay, Kowloon, Hong Kong, China

Supporting Information

ABSTRACT: As one of the most ordinary phenomena in nature, numerous pores on animal skins induce the growth of abundant hairs. In this study, cavities of a cellulose matrix were used as hard templates to lead the hair-inspired crystal growth of 12-hydroxyoctadecanoic acid (HOA) through hydrophobic–hydrophilic interface interaction, and short hair-like HOA crystals with a smooth surface were formed on cellulose films. In our findings, by using solvent evaporation induced crystallization, hydrophobic HOA grew along the hydrophilic cellulose pore wall to form regular vertical worm-like and pillar-like crystals with an average diameter of about 200 nm, depending on the experimental conditions and HOA concentration. The formation mechanism of the short hair-like HOA crystals as well as the structure and properties of the cellulose/HOA submicrometer composite films were studied. The pores of the cellulose matrix supplied not only cavities for the HOA crystals fixation but also hydrophilic shells to favor the vertical growth of the relatively hydrophobic HOA crystals. The cellulose/HOA submicrometer composite films exhibited high hydrophobicity, as a result of the formation of the solid/air composite surface. Furthermore, 4-(1,2,2-triphenylethenyl) benzoic acid, an aggregation-induced emission luminogen, was used to aggregate on the cellulose surface with HOA to emit and monitor the HOA crystal growth, showing bifunctional photoluminscence and self-cleaning properties. This work opens up a novel one-step pathway to design bio-inspired submicrometer materials by utilizing natural products, showing potential applications in self-cleaning optical devices.

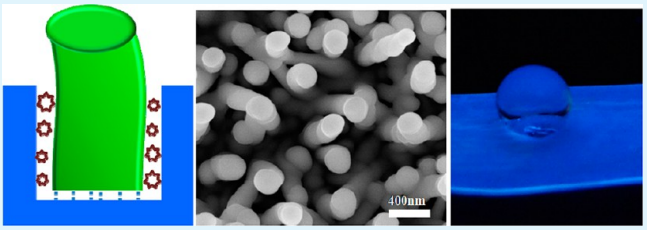

KEYWORDS: *hair-inspired crystal growth, hydrophobic–hydrophilic interface, porous cellulose matrix, aggregation-induced emission (AIE)*

1. INTRODUCTION

Recently, special and intriguing functionalities, such as the self-cleaning ability of animals and plants in nature, have attracted much attention as these functionalities would have wide applications in daily life.[1,2] Such functionalities are usually resulted from micro- and nano-scale structural features on the surfaces. For example, the micro-protrusion and nano-cilia endow lotus leaf with a self-cleaning ability,[1] the micro–nano hierarchical fibrous structure enables the water-strider to float on water,[3] the periodic spindle-knots nano-structure endows spider's web with a directional water-collecting ability in a moist environment.[4] Thus, such unique architecture can be resembled to mimic nature, and the resultant materials with similar functions can be used for research and industry production.[5−7] Lee et al. have studied the wing surface of *Cicada orni*, and they found that the self-cleaning ability of its wing is resulted from the vertical pillar structure. Therefore, they have used an aluminum sheet and nanoporous anodic aluminum oxide (AAO) as a replication template to construct a similar structure through heating and pressure-driven method, showing wide potential applications in optical and electronic devices.[8] These findings are very important in research and industry; however, this method is relatively complicated for the bio-inspired materials preparation, and the requirement for the apparatus is still high. Thus, a facile and low cost method is essential for successful fabrication of bio-inspired materials. Polymers can be used as hard templates to construct ordered and regular bio-inspired structures because of their facile processability, low cost and controllable architecture.[9−12] Cellulose, as the sustainable and most abundant biopolymer, has been easily converted into fibers, hydrogels, films and microspheres in our laboratory by using physical method in alkali/urea aqueous solvent.[13−17] In the previous findings, the cellulose gel sheets exhibited controllable homogenous porous structure, whose pore size ranged from 100 nm to several micrometers.[18] Such micro and nano pores on cellulose gels have been used for inorganic nanoparticles in situ synthesis, in-situ polymerization and crystal controllable growth,[19−23] showing that the porous

Received: March 28, 2014
Accepted: May 27, 2014
Published: May 27, 2014

cellulose matrix can be used as an ideal template. Moreover, the bio-inspired hydrophobic cellulose materials with special functionalities have been fabricated successfully by depositing various guest substances onto cellulose matrix.[24,25] A worthwhile endeavor would be to exploit new ways to construct bio-inspired materials by utilizing cellulose and an organic substance. As a natural product from castor oil, 12-hydroxyoctadecanoic (HOA) is an ordinary highly efficient gelator, and it can be used as detergents and lubricating greases in industrial applications.[26] Rogers et al. have studied the HOA molecular gels in solvents systematically, and they have found that HOA can form micrometer fibrillar structure in special solvents due to intermolecular hydrogen bonding interaction.[27−29] However, to the best of our knowledge, the regular vertical worm-like and pillar-like submicrometer crystal growth of HOA on a solid template through hydrophobic−hydrophilic interfaces interaction has never been reported.

As is known to us, abundant hair mainly consisted of "hard" keratin proteins can grow from the pores in the animal skin and its surface is relative smooth because of the incompatibility with skin pores (consisted of "soft" keratin proteins) due to the great difference in keratin species and content.[30,31] So, we are interested in utilizing the pores of the regenerated cellulose gel sheets for HOA crystal growth to form short hair-like crystals. Hydroxyls on the tail end of HOA can form hydrogen bonds with cellulose, and the hydrophobic−hydrophilic interfacial interaction led to the HOA crystal vertical and separate growth to form the "short hair-like structure". In addition, luminogens with aggregation-induced emission (AIE) characteristics have emerged as a novel class of fluorescent materials, which are nonluminescent or weakly fluorescent in the molecularly dissolved state, but are highly fluorescent in the aggregated state.[32,33] Tetraphenylethene (TPE) is a well-known AIE luminogen, as it is easy to prepare and functionalize. The hydrophobic nature of TPE or its derivative molecules may bind to the hydrophobic regions and become entrapped in the cavities of proteins and the hollow polysaccharide nanofibers through hydrophobic interactions,[34,35] causing the luminogen to fluoresce. In this work, we prepared a carboxylated TPE derivative as a fluorescent reporter to study the interaction between HOA and the surface of cellulose. 4-(1,2,2-Triphenylethenyl) benzoic acid (TPE-COOH) is easily soluble in ethanol and may interact with the hydrophobic long carbon chain in HOA through hydrophobic interaction. Using ethanol as the cosolvent for HOA and TPE-COOH dissolution to prepare blended solutions, where porous cellulose gel sheets with an average pore size of about 300 nm pore size were submerged. HOA crystals can grow homogeneously, orderly and controllably to form short hair-like crystals on the cellulose film surface, mimicking hair growth on animal skins. Thus, TPE-COOH could be used to monitor the HOA formation. Moreover, the bifunctional photoluminescent and hydrophobic cellulose films were constructed facilely through a one-step method, which sheds light on the design of self-cleaning optical devices.

2. EXPERIMENTAL SECTION

2.1. Materials. The cellulose sample (cotton linter pulp) was supplied by Hubei Chemical Fiber Co. Ltd. (Xiangfan, China). Its viscosity-average molecular weight (M_η) was determined by using an Ubbelohde viscometer in a LiOH/urea aqueous solution at 25 ± 0.05 °C and calculated from the equation $[\eta] = 3.72 \times 10^{-2} M_W^{0.77}$ to be 10.0×10^4 g/mol.[36] 4-Bromobenzophenone, *n*-butyllithium, diphenylmethane and *p*-toluene sulfonic acid monohydrate were purchased from Sigma-Aldrich. $LiOH{\cdot}H_2O$, urea and ethanol were supplied by Sinopharm Chemical Reagent Co. Ltd. Alkaline earth aluminate $[MAl_2O_4{:}Eu^{2+}$ (M = Ca, Sr)] were supplied by Dalian Luminglight Co. Ltd. Tetrahydrofuran (THF) was distilled from sodium benzophenone ketyl under nitrogen immediately prior to use. All chemicals and regents were commercially available and used as received without further purification unless further otherwise noted.

2.2. Preparation of Cellulose/HOA Composite Films. 8 wt % $LiOH{\cdot}H_2O$/15 wt % urea aqueous solutions were pre-cooled to −12.8 °C, and then the desired amounts of cellulose sample were added immediately. The cellulose was completely dissolved within 5 min with a stirring speed of about 1600 rpm to obtain a transparent 5 wt % cellulose solution. The cellulose solution was centrifuged to degas at 7200 rpm for 15 min, and then cast on a glass plate by glass tubes with two loops wrapped around its two sides to control the thickness of solution layers (about 0.2 mm). They were immediately coagulated with ethanol for 30 min to obtain cellulose gel sheets, which were first washed with running water and then exhaustively with deionized water to remove the excess urea and LiOH. The wet cellulose gel sheets were soaked repeatedly in an ethanol solution to remove the water. The resultant cellulose ethanol gel (RC E-gel), was then soaked in a HOA/ethanol solution to obtain cellulose/HOA composite ethanol gel (RCH E-gel). The RCH E-gels were dried at 25, 60 and 90 °C under atmospheric pressure or by vacuuming at −45 °C, and the resultant cellulose/HOA composite films were denoted as RCH. The RCH E-gels with 5 g/100 mL and 10 g/100 mL HOA concentrations through drying at 25, 60, 75 and 90 °C were coded as RCH5-25, RCH5-60, RCH5-75 and RCH5-90 as well as RCH10-25, RCH10-60, RCH5-75 and RCH10-90, respectively. The RCH E-gels with 5 g/100 mL and 10 g/100 mL HOA concentrations were vacuum-dried at low temperature and were denoted as RCH5 and RCH10, respectively. The film without HOA was coded as RC.

2.3. Preparation of Cellulose/HOA/TPE-COOH Composite Films. The details of the synthesis process for TPE-COOH are shown in the Supporting Information according to previous work,[37,38] and the synthesis route to TPE-COOH is shown as follows:

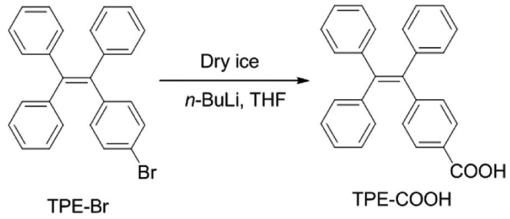

The desired amounts of HOA and TPE-COOH were dissolved in ethanol to prepare 5% HOA solutions with 5×10^{-4}, 2.5×10^{-4}, 1×10^{-4}, 0.5×10^{-4} and 0×10^{-4} M TPE-COOH concentrations. The RC E-gels were soaked in the above mixture solutions to prepare cellulose/HOA/TPE-COOH composite E-gel, which were subsequently dried at 60 °C and coded as RCHT5-5, RCHT5-2.5, RCHT5-1, RCHT5-0.5 and RCHT5-0, respectively.

2.4. Characterization. The morphologies of surface and cross-section for the RC and RCH composite films were observed by field emission scanning electron microscopy (FESEM, Zeiss, SIGMA). The acceleration voltage for the FESEM observation was 5 kV. The cellulose films or gel sheets were frozen in liquid nitrogen, immediately snapped and then freeze-dried for the SEM observation. The surface and cross-section of the films or gels were sputtered with gold and then observed. FT-IR spectra were carried out with a FT-IR spectrometer (1600, Perkin-Elmer Co., MA) in the wavelength range from 4000 to 400 cm^{-1}. The powdered and vacuum-dried samples were obtained, and the test specimens were prepared by the KBr disk method. Wide angle X-ray diffraction measurements were measured with a WAXD diffractometer (D8-Advance, Bruker, USA). The patterns with Cu Kα radiation (λ = 0.154 05 nm) at 40 kV and 30 mA were recorded in the region of 2θ from 5 to 40°, and the scanning rate was 2°/min. The samples were cut into powder and dried in a

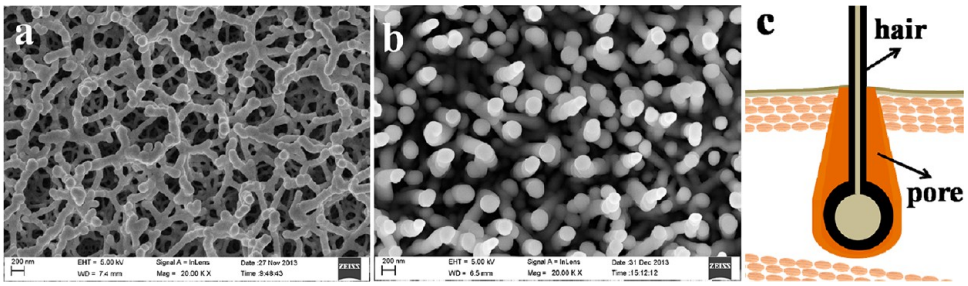

Figure 1. FESEM images of surface for freeze-dried 5 wt % cellulose gel (a) and cellulose film with HOA crystals (b), and scheme of the hair growth (c).

vacuum oven for 48 h before testing. Differential scanning calorimetry (DSC) experiments were performed on a NETZSCH DSC 200PC (NETZSCH, Germany) with a heating rate of 5°C/min. The temperature was controlled with liquid nitrogen, and the dried samples were put in a tightly sealed aluminum cell. The water contact angle was measured and calculated in dynamic mode on a Data Physics instrument (OCA20). One drop of water (2 μL) was put on the surface of the films with an automatic piston syringe and photographed. Photoluminescence (PL) spectra were measured on a Perkin-Elmer LS 55 spectrofluorometer with an excitation wavelength of 335 nm.

3. RESULTS AND DISCUSSION

3.1. Formation of Short Hair-Inspired HOA Crystals. From the cellulose solution dissolved in the LiOH/urea aqueous system with cooling, the regenerated cellulose gels were fabricated. Subsequently, the cellulose/HOA composite films were constructed by treating with HOA/ethanol solution and solvent evaporation. Figure 1 shows the FESEM images of the freeze-dried cellulose gel sheet (panel a) and RCH composite film (panel b), and the scheme of the hair growth (panel c). The corresponding statistical size histograms of the cellulose pores and diameter of HOA crystals are shown in Figure S1 (Supporting Information). Obviously, the cellulose surface exhibited a homogenous porous structure with an average pore size of about 300 nm. Usually, the cellulose pore size depends on cellulose concentration. The cellulose gel formation rate by using ethanol as a coagulation bath was much slower than that with acid or aqueous solution due to the relative slow diffusion into the aqueous system, so it could provide enough time for cellulose chain rearrangement and aggregation, resulting in a homogenous porous structure with smaller pore sizes. Thus, such a homogenous porous structure would provide an ideal matrix for crystal fixation and controllable growth.

As shown in Figure 1b, vertical pillar-like HOA crystals with an average diameter of about 200 nm appeared on the surface of the cellulose film. As mentioned in previous reports,[28,39] HOA can self-assemble into fibrillar crystals, where molecules formed cyclic dimers between carboxyl groups and hydrogen bonding interaction along the transverse axis favored longitudinal growth. In our findings, there were many longitudinal pores in the cellulose gel sheets, so the HOA crystals could aggregate and grow in the cavities of the cellulose matrix via solvent evaporation. It is noted that the self-aggregation of HOA is much stronger than its interaction with cellulose. Moreover, the HOA aggregates with a few hydroxyls on the tail end could form hydrogen bonds with cellulose to be fixed in the cellulose matrix, and the hydrophobic−hydrophilic interfacial interaction could induce the growth of the relatively hydrophobic HOA crystals along the pore wall of the hydrophilic cellulose separately. The HOA crystals had a circular cross-section and smooth surface, as a result of the incompatibility on the HOA−cellulose interface. The average diameter of the pillar-like crystals (about 200 nm) was smaller than that of the cellulose pore size (about 300 nm), further confirming that the hydrophobic−hydrophilic interfacial interaction existed between HOA and the cellulose matrix. The porous cellulose matrix supplied not only cavities for the HOA crystals fixation in the matrix through the hydrogen bonding interaction but also hydrophilic shells to favor the longitudinal and isolated growth of the HOA crystals. Figure 1c shows a schematic illustration of hair growth on the skin. Obviously, the growth of the HOA crystals was similar to "hair growth" on the skin. Therefore, this work would open up a novel one-step pathway to facilely design bio-inspired materials in the porous cellulose matrix by utilizing natural products.

3.2. Effects of Experimental Conditions on Structure and Morphology of HOA Crystals. Figure 2 shows WAXD

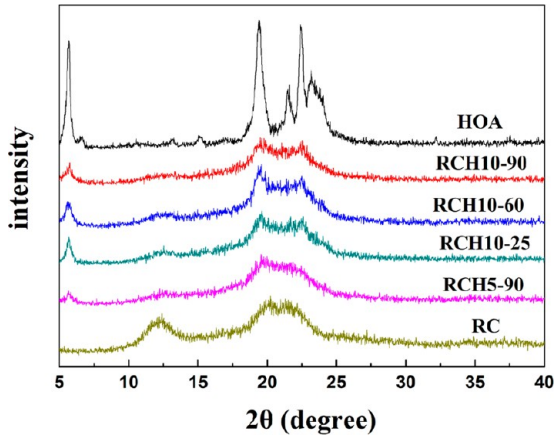

Figure 2. WAXD spectra of HOA, RCH10-90, RCH10-60, RCH10-25, RCH5-90 and RC.

spectra of HOA, RCH10-90, RCH10-60, RCH10-25 and RCH5-90. Three crystal peaks at 2θ = 12.2°, 19.9° and 21.3° for RC were assigned to crystal planes (110), ($1\bar{1}0$) and (200) of cellulose II, respectively.[40] The special peaks at 5.7, 19.4, 21.6 and 22.4°(23.3°) for HOA were assigned to the 15.2, 4.5, 3.9 and 3.8 Å subcell spacing, indicating triclinic parallel crystal form for raw HOA.[28] However, the peaks at 5.7 and 19.4° for HOA crystals grown on cellulose matrix were attributed to 15.2 and 4.3 Å subcell spacing (Figure 2, RCH10-90, RCH10-60, RCH10-25 and RCH5-90), showing hexagonal crystal formation and fibrillar aggregates characteristic.[28] The peak shape and intensity of the cellulose/HOA composite films varied with

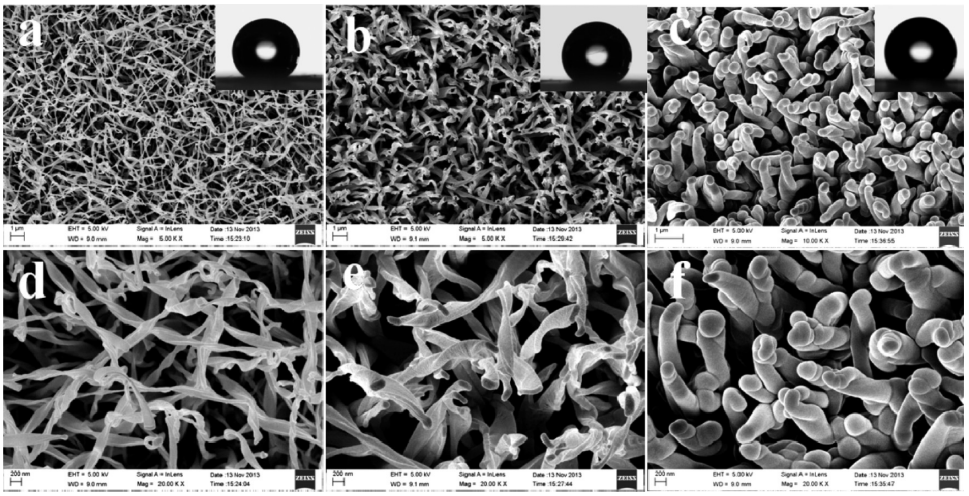

Figure 3. FESEM images of surface for RCH10-90 (a,d), RCH10-60 (b,e), RCH10-25 (c,f) films dried at different temperatures. Insets show the photographs of water droplets on each surface.

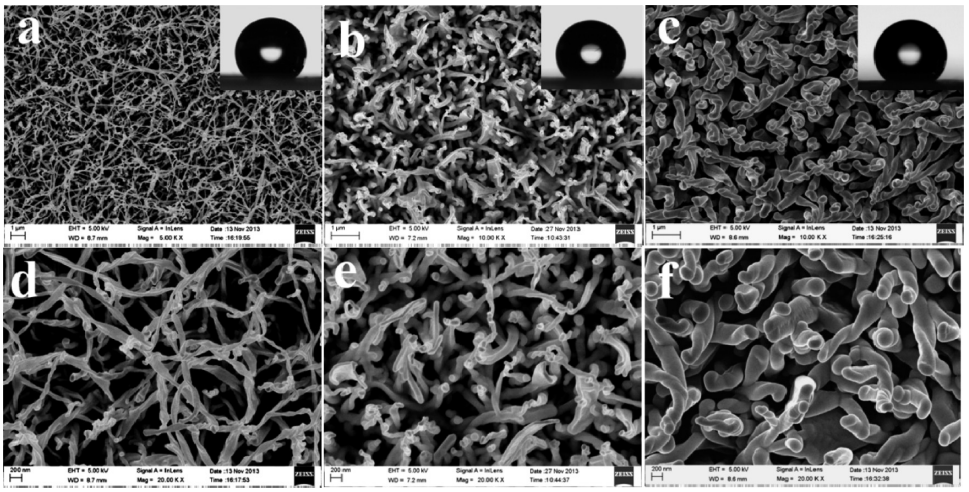

Figure 4. FESEM images of surface for RCH5-90 (a,d), RCH5-60 (b,e), RCH5-25 (c,f) films dried at different temperatures. Insets show the photographs of water droplets on each surface.

the drying temperature, so the crystal growth temperature affected the HOA crystal forms. Moreover, the peak intensity increased with HOA concentration. It was confirmed that utilizing the porous cellulose matrix for HOA crystal growth had feasibility.

Effects of drying temperature on the morphologies of HOA crystals grown on cellulose film were investigated. Figure 3 shows the SEM images of the surface morphologies on RCH films from different drying temperatures and the photographs of water droplets on each surface. Obviously, all the HOA crystals grown on the cellulose matrix exhibited a homogenous submicrometer fibrous structure. Such a structure was consistent with the longitudinal growth of HOA crystals.[39] Interestingly, the fibrous-network structure of HOA crystals appeared on the RCH10-90 cellulose films when the drying temperature was 90 °C (Figure 3a,d). The solvent evaporated very quickly at 90 °C, and the cellulose pores shrank rapidly at the same time, so abundant HOA came to the cellulose surface with rapid evaporation of ethanol, resulting in a fibrous-network structure. Vertical glass blade-like HOA crystals existed on the cellulose film at 60 °C, and the size of HOA crystals was bigger than that at 90 °C. Especially, there were worm-like HOA crystals grown on the cellulose matrix at 25 °C, and the crystal size was much bigger than that at 60 °C and 90 °C. The solvent evaporation was slowest at this temperature, and the cellulose pore shrinkage was much slower than others, so the long free-growth time and relatively large pore space led to the formation of perfect worm-like HOA crystals with smooth surface. Apparently, these HOA crystals changed the cellulose surface morphology. The interspaces among HOA crystals could trap abundant air, resulting in a solid/air composite surface to increase the hydrophobicity.[41] Thus, high hydrophobic cellulose films (water contact angles were above 140°) with HOA crystals were fabricated here. The morphologies of raw HOA (a and b) and HOA reproduced from 10 wt % HOA/ethanol solution without porous cellulose matrix by evaporation at 25 °C (c and d) are shown as the control in Figure S2 (Supporting Information). Obviously, the HOA did not exhibit the regular fibrillar structure, indicating the important role of cellulose pores on the regular submicrometer HOA crystal formation. Usually, the crystal growth concentration affects its micro and macro structure.[42] So the HOA crystal morphology grown on cellulose matrix from lower HOA concentration at different temperatures was also studied. Figure 4 shows the

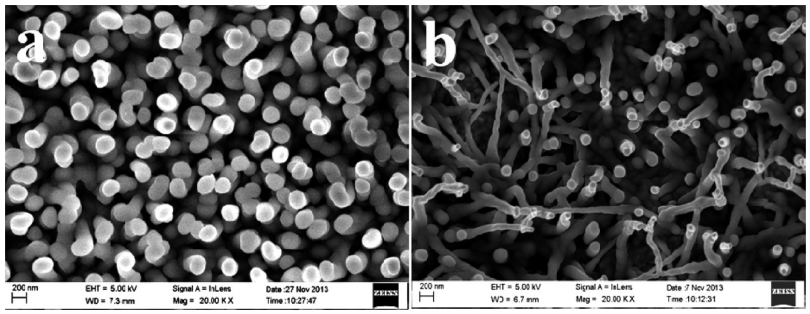

Figure 5. FESEM images of the surface for RCH10 (a) and RCH5 (b) by vacumming at −45 °C.

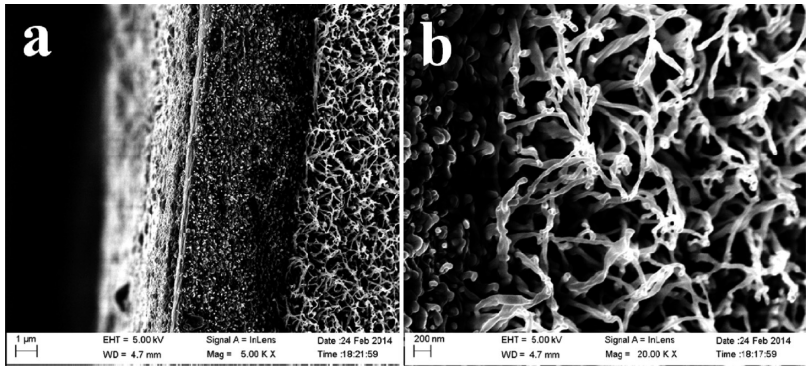

Figure 6. SEM images of the cross-section and interface between HOA crystals and cellulose film for RCH5-75 (a); panel b is the enlargement of panel a.

Scheme 1. Procedure and Mechanism of the HOA Crystal Growth on Cellulose Gel

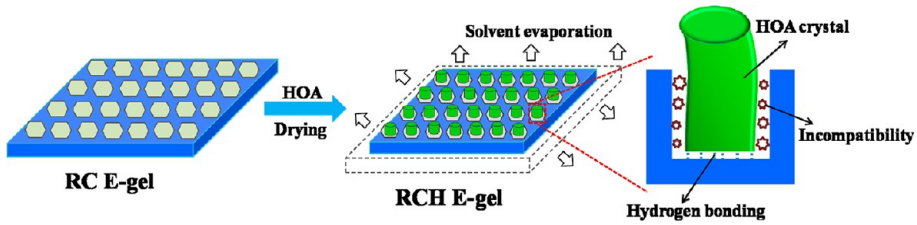

SEM images of the surface morphologies for RCH films with 5% HOA concentration and photographs of the water droplets on each surface. Clearly, similar homogenous submicrometer fibrous structures were obtained. However, the crystal size reduced with the decrease of HOA concentration. The fibrous network structure of HOA crystals also appeared on the cellulose film at 90 °C with lower HOA concentrations, but the corresponding fiber diameter was much smaller, resulting in larger interspaces among the crystals. At 60 °C treatment, HOA crystal fibers with two different sizes appeared on the cellulose film (Figure 4b,e), the larger fiber was similar to that grown at 60 °C with a 10 wt % HOA concentration (Figure 3b,e), while the smaller fiber resembled that grown at 90 °C (Figure 4a,d). This phenomenon indicated that the HOA concentration affected its crystal morphology, which might be caused by relative insufficient HOA amount at 60 °C with this concentration. The worm-like crystals with relative smaller size were also obtained at 25 °C(Figure 4c,f). The cellulose matrix couldn't capture HOA crystals tightly as those with higher HOA concentrations (Figure 3c,f) because the relatively large cellulose pores were difficult to fit small HOA crystals well, so part of the HOA crystals leaned. Relatively high HOA concentrations favored the fixation of HOA crystals in cellulose matrix and the formation of crystals with large diameters.

Besides heating, vacuuming can also be used to evaporate solvents rapidly, and a low-temperature vacuuming method was used here. Figure 5 shows the HOA crystal morphologies from the vacuuming process at −45 °C. At high vacuuming, ethanol could evaporate quickly, so HOA nucleation and growth occurred very rapidly. Vertical pillar-like HOA crystals appeared both on the surfaces of RCH10 and RCH5 (Figure 5a,b), and the HOA crystals on RCH10 were much denser than that on RCH5. Furthermore, the diameter of the HOA pillar-like crystals on RCH10 was much larger than that on RCH5. Thus, the diameter and distribution of HOA crystals could be adjusted by changing the HOA concentrations. Interestingly, such vertical pillar-like HOA crystal structure resembled that on the wing surface of *Cicada orni*,[8] so we could fulfill the HOA crystal ordered growth to construct a bio-inspired structure through a facile method. Figure 6 shows the SEM images of the cross-section of RCH5-75 film and the interface between HOA crystals and the cellulose film. Apparently, the HOA crystals distributed mainly on the one side of the cellulose film, and there were only a few HOA crystals on the cross-section and the other side (Figure 6a). This phenomenon was mainly

caused by the HOA migration to the one side of the cellulose film via solvent evaporation. Once the solvent evaporated completely, HOA crystals stopped growing outwards on the whole, the unmigrated small amount of HOA was left in the cellulose matrix, which could form crystals inside the cellulose film. Calculated from Figure 6b, the length of HOA crystal fiber grown from cellulose matrix was about 1 μm. Thus, we can control the HOA crystal growth and prepare HOA crystal fibers simply by using a cellulose template and solvent evaporation induced crystallization method. Meanwhile, the HOA crystals could prevent the direct contact between cellulose and water droplets, resulting in hydrophobicity enhancement. Obviously, the one-side high hydrophobic and one-side hydrophilic cellulose film could be fabricated easily. Such a cellulose film shows potential applications in medical dressing, because the hydrophobic side can be used for water repellent and self-cleaning, whereas the other hydrophilic side can absorb sweat inside to keep the skin dry.[43]

On the basis of the results mentioned above, a schematic presentation for the HOA crystal growth process on a cellulose matrix is proposed in Scheme 1. During the solvent evaporation process, the HOA migrated to the one side of the cellulose gel sheet. Subsequently, HOA could crystallize outwardly along the cellulose pores, and grow homogeneously and vertically on the cellulose matrix. The tail end of HOA crystals was fixed in the bottom of the cellulose pores through hydrogen bonding interaction between cellulose and a few hydroxyls in the tail of HOA. Therefore, this was a bio-inspired process, and the cellulose porous structure could be used as a template for regular submicrometer crystal growth.

3.3. Physical Properties of the Cellulose/HOA Submicrometer Composite Films. Figure 7 shows the FT-IR

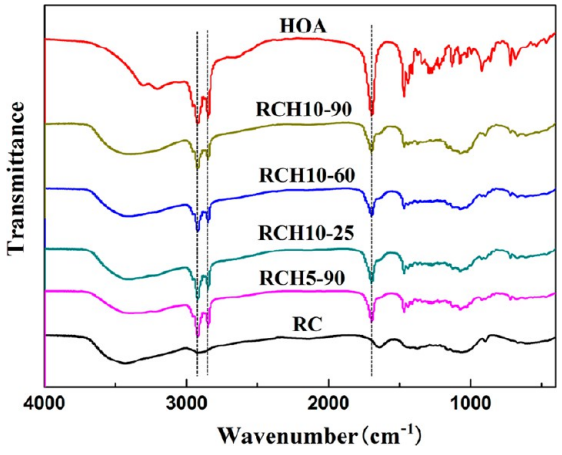

Figure 7. FT-IR spectra of HOA, RCH10-90, RCH10-60, RCH10-25, RCH5-90 and RC.

spectra of the HOA, RCH10-90, RCH10-60, RCH10-25, RCH5-90 and RC films. The location, band width and shape of the HOA absorption band depend on the HOA dimer formed by hydrogen bonding through intermolecular carbonyl.[44] The asymmetric ($\nu_{as}(CH_2)$), symmetric ($\nu_s(CH_2)$) methylene vibration and carbonyl absorption of carboxylic acid dimer ($\nu_{C=O}$) peaks for HOA appeared clearly at 2918, 2860, and 1702 cm^{-1}, respectively. The zones of 1415, 1289, and 934 cm^{-1} were attributed to hydroxyl proton resonance absorbing (δ_{OH}), C−O stretching vibration (ν_{C-O}), and the off-plate vibration bands of O−H of HOA dimer, respectively. The shoulder-absorption band at 2480−2715 cm^{-1} was caused by the combination of the C−O stretching vibration, the O−H deforming vibration and the frequency doubling of the C−O stretching−contracting vibration frequency. The bands of the RC and RCH films at 3320−3518 cm^{-1} were attributed to stretching vibrations for hydroxyl groups of cellulose. Compared with RC, the peaks for RCH10-90, RCH10-60, RCH10-25 and RCH5-90 films shortened and shifted to higher wavenumbers, indicating the existence of strong intermolecular hydrogen bonding interactions between cellulose and HOA. The FT-IR results indicated that there was dipole−dipole interaction between the carboxylic groups of HOA.[45] Moreover, the HOA crystal growth on the cellulose matrix was a physical process; no chemical reaction occurred.

The HOA crystal morphologies grown from a cellulose matrix at different temperatures and concentrations may be related to their thermal properties, so DSC was employed to study the melting temperature and crystallization behavior. Figure 8 shows the DSC curves for the RC and RCH films. The

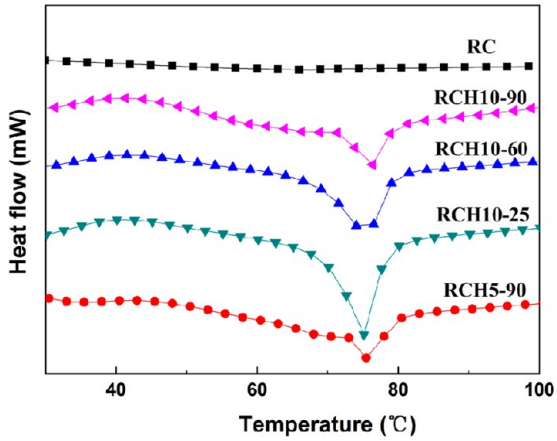

Figure 8. DSC curves of RCH10-90, RCH10-60, RCH10-25, RCH5-90 and RC.

melting temperature (T_m) for RCH10-90, RCH10-60 and RCH10-25 was 76.5, 75.5 and 75.0 °C, respectively. This result revealed that the structure of crystals formed from different drying temperature was different to some extent, and the T_m decreased with a decrease of the drying temperature, coinciding with results from WAXD and FESEM. Moreover, the melting enthalpy increased with the decrease of drying temperature as a result of perfect crystallization at low temperature. To test the stability of the prepared surfaces and morphologies, the RCH5-75 films were rinsed with water (ethanol) and heat-treated at 100 °C. The resultant morphologies are shown in Figure S3 (Supporting Information), the morphology for RCH5-75 remained almost the same after water flush (Figure S3a,b, Supporting Information), showing good stability against water. Interestingly, the jointed submicrometer HOA fibers appeared on the RCH5-75 film after being rinsed with ethanol, which was caused by partial dissolution by ethanol and recrystallization. The submicrometer HOA fibers disappeared, and micro HOA fibers appeared after heat treatment (panel d) because the resultant abundant liquid HOA could crystallize spontaneously with cooling, further confirming the role of cellulose pores on the formation of submicrometer HOA fibers. Therefore, the composite films exhibited certain stability

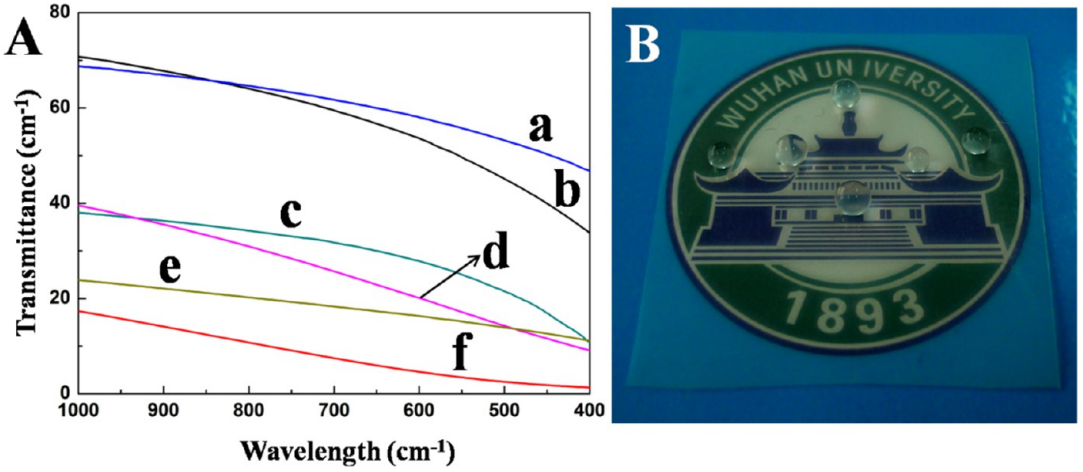

Figure 9. UV−vis spectra of RCH5-90 (a), RCH5-60 (b), RCH5-25 (e), RCH10-90 (c), RCH10-60 (d) and RCH10-25 (f) (A); photograph of RCH5-90 covered on a university badge with water droplets (B).

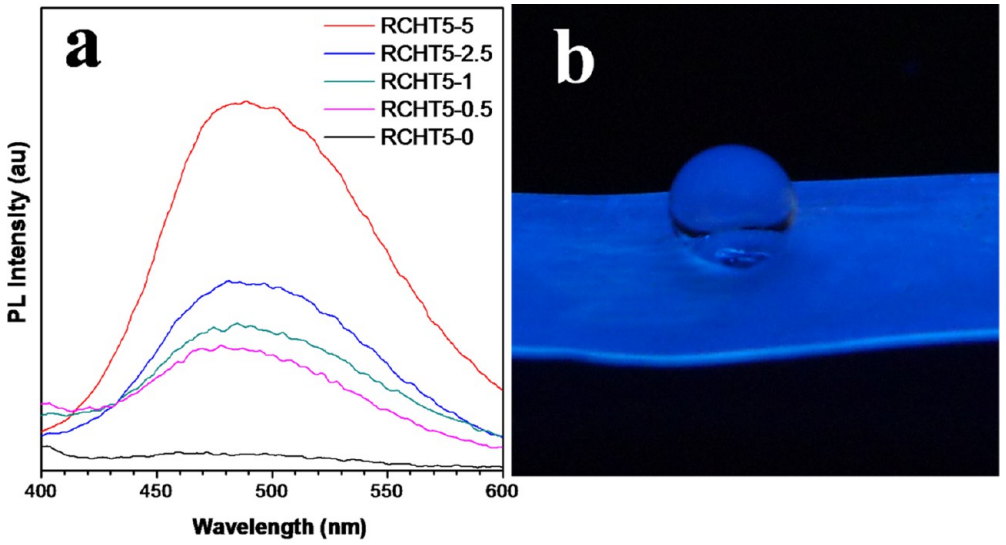

Figure 10. PL spectra of the RC films from 5 wt % HOA/ethanol solutions with different TPE-COOH concentrations: 0, 0.5, 1, 2.5 and 5 (10^{-4} M) (a) and the photograph of RCHT5-5 with a water droplet under an UV lamp (b).

against water and ethanol, which could meet the requirement of our daily usage.

Figure 9 shows UV−vis spectra of RCH5-90, RCH5-60, RCH5-25, RCH10-90, RCH10-60 and RCH10-25. The RCH films exhibited certain transparency, and increased with the increase of drying temperature and decrease of HOA concentration (Figure 9A). This indicated that the transparency was in inverse proportion to crystal size. Therefore, a cellulose film with bigger HOA crystals, compared with that with smaller crystals, exhibited a decrease in transparency due to larger light loss from light reflection and refraction. The RCH5-90 displayed the best transparency (58% at 600 nm), as shown in Figure 9B.

3.4. Aggregation-Induced Emission (AIE) of Submicrometer Cellulose Films. Figure 10 shows the PL spectra of the cellulose/HOA/TPE-COOH composite films (panel a) and the photograph of RCHT5-5 with a water droplet under an UV lamp (panel b). Obviously, the cellulose/HOA submicrometer composite film exhibited almost no fluorescence, and the PL intensity increased with the TPE-COOH concentration. Generally, TPE-COOH is almost nonemissive when molecularly dissolved in solution, but TPE-COOH could combine with HOA through hydrophobic interaction and migrate to the cellulose film surface with the solvent evaporation, so it could aggregate and distribute evenly on cellulose film surface with the HOA crystal growth, resulting in emitting efficiently. The submicrometer composite film with low TPE-COOH concentration was weak-emissive due to the relative far apart among TPE-COOH molecules, so intramolecular rotations (IR) could consume part of energy to decrease the PL intensity. The AIE molecules packed closely with increasing TPE-COOH concentration, and the aggregation was much more severely to restrict the IR efficiently,[32,46−48] resulting in much higher PL intensity. The RCHT5-5 composite film displayed blue emission under UV light excitation. Moreover, the RCHT5-5 exhibited high hydrophobicity. The excellent hydrophobicity and certain self-cleaning ability of the submicrometer composite films are shown in the Figure S4 and the video (see the Supporting Information). To demonstrate the effect of solvent evaporation on HOA crystal formation and diffusion of HOA, one edge of cellulose/HOA/TPE-COOH gel was covered with plastic sheet to prevent the solvent evaporation.

The resultant composite film is shown in Figure S5 (Supporting Information). Interestingly, the covered edge was hydrophilic without fluorescence, while the uncovered area was hydrophobic and emitted strongly, indicating that the hydrophobic interaction existed between HOA and TPE-COOH. In addition, TPE-COOH could be used to monitor the HOA formation based on hydrophobic interaction. Therefore, we have fabricated bifunctional photoluminescent/hydrophobic cellulose materials through a one-step method, which have potential applications in optoelectronic, anticounterfeiting packaging, displaying and functional packaging areas.[49]

4. CONCLUSIONS

The porous cellulose gel sheet was found to be an ideal matrix for uniform crystal growth of 12-hydroxyoctadecanoic acid (HOA) and a template for biomimicking. By using solvent evaporation induced crystallization, vertical worm-like and pillar-like crystals of HOA were constructed on the cellulose film surface, resembling the short hair-growth. The porous cellulose matrix supplied not only cavities for the HOA crystals fixation but also hydrophilic shells to favor the longitudinal and isolated growth of the HOA crystals. The HOA aggregates with a few hydroxyls on the tail end could form hydrogen bonds with cellulose to be fixed in the cellulose matrix. The hydrophobic−hydrophilic interfacial interaction could induce the growth of the relatively hydrophobic HOA crystals along the pore wall of the hydrophilic cellulose separately, which exhibited a smooth surface. The HOA crystal morphologies can be controlled by changing the temperature and HOA concentration, and the perfect worm-like crystals could be fabricated by adjusting the experimental conditions. The cellulose/HOA submicrometer composite films exhibited high hydrophobicity with certain self-cleaning ability. Furthermore, the bifunctional photoluminescent and hydrophobic cellulose/HOA/TPE-COOH films were successfully fabricated by combining TPE-COOH with HOA through hydrophobic interaction to migrate onto the cellulose film surface, resulting in efficiently emitting. This work opens up a novel one-step pathway to facilely design bio-inspired materials in a porous cellulose matrix by utilizing natural products, to resemble short hair-growth on the skin in nature.

■ ASSOCIATED CONTENT

Supporting Information

Synthesis process of TPE-COOH. Statistical size histograms of the cellulose pores and diameter of HOA crystals. FESEM images of raw HOA and HOA reproduced from 10 wt % HOA/ethanol solution without a porous cellulose matrix by treating at 25 °C. FESEM images of surface for RCH5-75 film, RCH5-75 films rinsed with water and ethanol, and heated at 100 °C. Photographs of the composite cellulose film with alkaline earth dye as "dust" before and after being dripped with a drop of water under an UV lamp. Video of excellent hydrophobicity and certain self-cleaning ability. Photograph of RCHT5-2.5 with water droplets under an UV lamp. This material is available free of charge via the Internet at http://pubs.acs.org.

■ AUTHOR INFORMATION

Corresponding Authors

*L. Zhang. Phone: +86-27-87219274. Fax: +86-27-68762005. E-mail: zhangln@whu.edu.cn.

*B. Z. Tang. E-mail: tangbenz@ust.hk.

Notes

The authors declare no competing financial interest.

■ ACKNOWLEDGMENTS

This work was supported by National Basic Research Program of China (973 Program, 2010CB732203, 2013CB834701), the Major Program of National Natural Science Foundation of China (21334005) and the National Natural Science Foundation of China (20874079, 81171480). The Research Grants Council of Hong Kong (N_HKUST620/11), and Guangdong Innovative Research Team Program (201101C0105067115).

■ REFERENCES

(1) Sun, T.; Feng, L.; Gao, X.; Jiang, L. Bioinspired Surfaces with Special Wettability. *Acc. Chem. Res.* **2005**, *38*, 644−652.

(2) Roach, P.; Shirtcliffe, N. J.; Newton, M. I. Progess in Superhydrophobic Surface Development. *Soft Matter* **2008**, *4*, 224−240.

(3) Gao, X.; Jiang, L. Biophysics: Water-Repellent Legs of Water Striders. *Nature* **2004**, *432*, 36−36.

(4) Zheng, Y.; Bai, H.; Huang, Z.; Tian, X.; Nie, F.-Q.; Zhao, Y.; Zhai, J.; Jiang, L. Directional Water Collection on Wetted Spider Silk. *Nature* **2010**, *463*, 640−643.

(5) Malvadkar, N. A.; Hancock, M. J.; Sekeroglu, K.; Dressick, W. J.; Demirel, M. C. An Engineered Anisotropic Nanofilm with Unidirectional Wetting Properties. *Nat. Mater.* **2010**, *9*, 1023−1028.

(6) Geim, A.; Dubonos, S.; Grigorieva, I.; Novoselov, K.; Zhukov, A.; Shapoval, S. Y. Microfabricated Adhesive Mimicking Gecko Foot-Hair. *Nat. Mater.* **2003**, *2*, 461−463.

(7) Lee, H.; Lee, B. P.; Messersmith, P. B. A Reversible Wet/Dry Adhesive Inspired by Mussels and Geckos. *Nature* **2007**, *448*, 338−341.

(8) Lee, W.; Jin, M.-K.; Yoo, W.-C.; Lee, J.-K. Nanostructuring of a Polymeric Substrate with Well-Defined Nanometer-Scale Topography and Tailored Surface Wettability. *Langmuir* **2004**, *20*, 7665−7669.

(9) Thomas, A.; Goettmann, F.; Antonietti, M. Hard Templates for Soft Materials: Creating Nanostructured Organic Materials. *Chem. Mater.* **2008**, *20*, 738−755.

(10) Bonderer, L. J.; Studart, A. R.; Gauckler, L. J. Bioinspired Design and Assembly of Platelet Reinforced Polymer Films. *Science* **2008**, *319*, 1069−1073.

(11) Ma, M.; Guo, L.; Anderson, D. G.; Langer, R. Bio-inspired Polymer Composite Actuator and Generator Driven by Water Gradients. *Science* **2013**, *339*, 186−189.

(12) Bleek, K.; Taubert, A. New Developments in Polymer-Controlled, Bioinspired Calcium Phosphate Mineralization from Aqueous Solution. *Acta Biomater.* **2013**, *9*, 6283−6321.

(13) Cai, J.; Zhang, L.; Zhou, J.; Qi, H.; Chen, H.; Kondo, T.; Chen, X.; Chu, B. Multifilament Fibers Based on Dissolution of Cellulose in NaOH/Urea Aqueous Solution: Structure and Properties. *Adv. Mater.* **2007**, *19*, 821−825.

(14) He, M.; Zhao, Y.; Duan, J.; Wang, Z.; Chen, Y.; Zhang, L. Fast Contact of Solid-Liquid Interface Created High Strength Multi-Layered Cellulose Hydrogels with Controllable Size. *ACS Appl. Mater. Interfaces* **2014**, *6*, 1872−1878.

(15) Chang, C.; He, M.; Zhou, J.; Zhang, L. Swelling Behaviors of pH-and Salt-Responsive Cellulose-Based Hydrogels. *Macromolecules* **2011**, *44*, 1642−1648.

(16) Luo, X.; Liu, S.; Zhou, J.; Zhang, L. In Situ Synthesis of Fe_3O_4/Cellulose Microspheres with Magnetic-Induced Protein Delivery. *J. Mater. Chem.* **2009**, *19*, 3538−3545.

(17) Qi, H.; Chang, C.; Zhang, L. Properties and Applications of Biodegradable Transparent and Photoluminescent Cellulose Films Prepared Via a Green Process. *Green Chem.* **2008**, *11*, 177−184.

(18) Cai, J.; Wang, L.; Zhang, L. Influence of Coagulation Temperature on Pore Size and Properties of Cellulose Membranes

Prepared from NaOH−Urea Aqueous Solution. *Cellulose* **2007**, *14*, 205−215.
(19) Cai, J.; Liu, S.; Feng, J.; Kimura, S.; Wada, M.; Kuga, S.; Zhang, L. Cellulose−Silica Nanocomposite Aerogels by In Situ Formation of Silica in Cellulose Gel. *Angew. Chem., Int. Ed.* **2012**, *124*, 2118−2121.
(20) Liu, S.; Zhang, L.; Zhou, J.; Xiang, J.; Sun, J.; Guan, J. Fiberlike Fe_2O_3 Macroporous Nanomaterials Fabricated by Calcinating Regenerate Cellulose Composite Fibers. *Chem. Mater.* **2008**, *20*, 3623−3628.
(21) He, M.; Xu, M.; Zhang, L. Controllable Stearic Acid Crystal Induced High Hydrophobicity on Cellulose Film Surface. *ACS Appl. Mater. Interfaces* **2013**, *5*, 585−591.
(22) Shi, Z.; Gao, H.; Feng, J.; Ding, B.; Cao, X.; Kuga, S.; Wang, Y.; Zhang, L.; Cai, J. In Situ Synthesis of Robust Conductive Cellulose/Polypyrrole Composite Aerogels and Their Potential Application in Nerve Regeneration. *Angew. Chem., Int. Ed.* **2014**, *53*, 5380−5384.
(23) Li, W.; Wu, Y.; Liang, W.; Li, B.; Liu, S. Reduction of the Water Wettability of Cellulose Film Through Controlled Heterogeneous Modification. *ACS Appl. Mater. Interfaces* **2014**, *6*, 5726−5734.
(24) Jin, C.; Yan, R.; Huang, J. Cellulose Substance with Reversible Photo-Responsive Wettability by Surface Modification. *J. Mater. Chem.* **2011**, *21*, 17519−17525.
(25) Jin, C.; Jiang, Y.; Niu, T.; Huang, J. Cellulose-Based Material with Amphiphobicity to Inhibit Bacterial Adhesion by Surface Modification. *J. Mater. Chem.* **2012**, *22*, 12562−12567.
(26) Eloundou, J. P.; Girard-Reydet, E.; Gérard, J.-F.; Pascault, J.-P. Calorimetric and Rheological Studies of 12-Hydroxystearic acid/Digycidyl Ether of Bisphenol A blends. *Polym. Bull.* **2005**, *53*, 367−375.
(27) Lam, R. S. H.; Rogers, M. A. Experimental Validation of the Modified Avrami Model for Non-isothermal Crystallization Conditions. *CrystEngComm* **2011**, *13*, 866−875.
(28) Wu, S.; Gao, J.; Emge, T. J.; Rogers, M. A. Solvent-Induced Polymorphic Nanoscale Transitions for 12-Hydroxyoctadecanoic Acid Molecular Gels. *Cryst. Growth Des.* **2013**, *13*, 1360−1366.
(29) Rogers, M. A.; Marangoni, A. G. Solvent-Modulated Nucleation and Crystallization Kinetics of 12-Hydroxystearic Acid: A Non-isothermal Approach. *Langmuir* **2009**, *25*, 8556−8566.
(30) Hearle, J. A Critical Review of the Structural Mechanics of Wool and Hair Fibres. *Int. J. Biol. Macromol.* **2000**, *27*, 123−138.
(31) Powell, B. C.; Rogers, G. E. In *Formation and Structure of Human Hair*; Jolles, P. H., Zahn, H., Hocker, H., Eds.; Birkhaüser Verlag: Berlin, 1995; pp 59−148.
(32) Hong, Y.; Lam, J. W.; Tang, B. Z. Aggregation-Induced Emission: Phenomenon, Mechanism and Applications. *Chem. Commun.* **2009**, 4332−4353.
(33) Hong, Y.; Lam, J. W.; Tang, B. Z. Aggregation-Induced Emission. *Chem. Soc. Rev.* **2011**, *40*, 5361−5388.
(34) Hong, Y.; Meng, L.; Chen, S.; Leung, C. W. T.; Da, L.-T.; Faisal, M.; Silva, D.-A.; Liu, J.; Lam, J. W. Y.; Huang, X. Monitoring and Inhibition of Insulin Fibrillation by a Small Organic Fluorogen with Aggregation-Induced Emission Characteristics. *J. Am. Chem. Soc.* **2012**, *134*, 1680−1689.
(35) Xu, S.; Lin, Y.; Huang, J.; Li, Z.; Xu, X.; Zhang, L. Construction of High Strength Hollow Fibers by Self-Assembly of a Stiff Polysaccharide with Short Branches in Water. *J. Mater. Chem. A* **2013**, *1*, 4198−4206.
(36) Cai, J.; Liu, Y.; Zhang, L. Dilute Solution Properties of Cellulose in LiOH/Urea Aqueous System. *J. Polym. Sci., Part B: Polym. Phys.* **2006**, *44*, 3093−3101.
(37) Song, Z.; Hong, Y.; Kwok, R. T.; Lam, J. W.; Liu, B.; Tang, B. Z. A Dual-Mode Fluorescence "Turn-on" Biosensor Based on an Aggregation-Induced Emission Luminogen. *J. Mater. Chem. B* **2014**, *2*, 1717−1723.
(38) Zhou, X.; Li, H.; Chi, Z.; Zhang, X.; Zhang, J.; Xu, B.; Zhang, Y.; Liu, S.; Xu, J. Piezofluorochromism and Morphology of a New Aggregation-Induced Emission Compound Derived from Tetraphenylethylene and Carbazole. *New J. Chem.* **2012**, *36*, 685−693.
(39) Grahame, D. A.; Olauson, C.; Lam, R. S.; Pedersen, T.; Borondics, F.; Abraham, S.; Weiss, R. G.; Rogers, M. A. Influence of Chirality on the Modes of Self-Assembly of 12-Hydroxystearic Acid in Molecular Gels of Mineral Oil. *Soft Matter* **2011**, *7*, 7359−7365.
(40) Isogai, A.; Usuda, M.; Kato, T.; Uryu, T.; Atalla, R. H. Solid-State CP/MAS Carbon-13 NMR Study of Cellulose Polymorphs. *Macromolecules* **1989**, *22*, 3168−3172.
(41) Crick, C. R.; Parkin, I. P. Preparation and Characterisation of Super-Hydrophobic Surfaces. *Chem.—Eur. J.* **2010**, *16*, 3568−3588.
(42) Athauda, T. J.; Hari, P.; Ozer, R. R. Tuning Physical and Optical Properties of ZnO Nanowire Arrays Grown on Cotton Fibers. *ACS Appl. Mater. Interfaces* **2013**, *5*, 6237−6246.
(43) Sarkar, M. K.; He, F.; Fan, J. Differential Superhydrophobicity and Hydrophilicity on a Thin Cellulose Layer. *Thin Solid Films* **2010**, *518*, 5033−5039.
(44) Tang, Z.; Liu, A.; Chen, Z. Study on Performance of Colloidal Mixtures Consisted of Stearic acid and $Na_2HPO_4{\cdot}12H_2O$ for Use as Phase Change Materials of Thermal Energy Storage. *Energy Convers. Manage.* **2010**, *51*, 1459−1463.
(45) Tamura, T.; Ichikawa, M. Effect of Lecithin on Organogel Formation of 12-Hydroxystearic Acid. *J. Am. Oil Chem. Soc.* **1997**, *74*, 491−495.
(46) Chen, J.; Law, C. C.; Lam, J. W.; Dong, Y.; Lo, S. M.; Williams, I. D.; Zhu, D.; Tang, B. Z. Synthesis, Light Emission, Nanoaggregation, and Restricted Intramolecular Rotation of 1,1-Substituted 2,3,4,5-Tetraphenylsiloles. *Chem. Mater.* **2003**, *15*, 1535−1546.
(47) Zhao, Z.; Chen, S.; Lam, J. W.; Jim, C. K.; Chan, C. Y.; Wang, Z.; Lu, P.; Deng, C.; Kwok, H. S.; Ma, Y. Steric Hindrance, Electronic Communication, and Energy Transfer in the Photo- and Electroluminescence Processes of Aggregation-Induced Emission Luminogens. *J. Phys. Chem. C* **2010**, *114*, 7963−7972.
(48) Tong, H.; Hong, Y.; Dong, Y.; Häussler, M.; Li, Z.; Lam, J. W.; Dong, Y.; Sung, H. H.-Y.; Williams, I. D.; Tang, B. Z. Protein Detection and Quantitation by Tetraphenylethene-Based Fluorescent Probes with Aggregation-Induced Emission Characteristics. *J. Phys. Chem. B* **2007**, *111*, 11817−11823.
(49) Hou, L.; Wang, C.; Chen, L.; Chen, S. Multiple-Structured Nanocrystals towards Bifunctional Photoluminescent-Superhydrophobic Surfaces. *J. Mater. Chem.* **2010**, *20*, 3863−3868.